

See discussions, stats, and author profiles for this publication at: <https://www.researchgate.net/publication/318284699>

# An Affordable Stroboscopic Imaging Technique For Studying Liquid Droplet Shape Oscillations

Article · April 2017

CITATIONS

2

READS

281

4 authors:



**Alexander Pimpas**

Sofia University "St. Kliment Ohridski"

1 PUBLICATION 2 CITATIONS

[SEE PROFILE](#)



**Pavlin Tsonev**

Sofia University "St. Kliment Ohridski"

1 PUBLICATION 2 CITATIONS

[SEE PROFILE](#)



**Andreana Andreeva**

Sofia University "St. Kliment Ohridski"

20 PUBLICATIONS 37 CITATIONS

[SEE PROFILE](#)



**Nikolay Zografov**

Sofia University "St. Kliment Ohridski"

18 PUBLICATIONS 32 CITATIONS

[SEE PROFILE](#)

Some of the authors of this publication are also working on these related projects:



Aprovechamiento sustentable del cultivo de la piña (*Ananas comosus* L. Merrill) en México [View project](#)



## An Affordable Stroboscopic Imaging Technique For Studying Liquid Droplet Shape Oscillations

Alexander Pimpas<sup>1</sup>, Pavlin Tsonev<sup>1</sup>, Andreana Andreeva<sup>1</sup>, and Nikolay Zografov<sup>1</sup>

<sup>1</sup>Faculty of Physics, Sofia University “St. Kliment Ohridski”, 5 J. Bourchier, Blvd, 1164 Sofia, Bulgaria.

**Abstract.** A simple and affordable stroboscopic imaging technique for studying liquid droplet shape oscillations is proposed. It's based on regular PC sound card I/O capabilities, a standard web camera, used as an imaging device, and free software. The sound card is used as a functional generator sending waveform signals to the light source and is simultaneously used as an oscilloscope. The webcam captures images or videos that can be obtained and either analyzed in real time or saved for further analysis. In the present work, we describe the theoretical bases, technical details, the capabilities and limitations of the developed stroboscopic technique. Experimental results of study on shape oscillations up to 300 Hz of millimeter-sized pendant or sessile water droplets are reported.

**Keywords:** Stroboscopic imaging, Droplet, Oscillations, Surface tension.

### 1. INTRODUCTION

Many modern studies in the field of physics and chemistry are based on the analysis of shape oscillations of liquid droplets and bubbles (Milne et al., 2014; Zografov et al., 2014). The main applications of these studies are in the field of surface tension measurements, in examining viscoelastic properties of liquids (Meier et al., 2000; Zografov et al., 2013) and in fundamental studies (Noblin et al., 2005). In the vast majority of experiments, the shape oscillations are studied by imaging techniques, demanding expensive high-speed video cameras (Oh et al. 2008; Tran et al. 2011; Mettu et al. 2012; Deepu et al., 2014 ; Shin et al, 2014). Compared to high-speed cameras, stroboscopic techniques are less often used, but even then, expensive components and a DSLR photo camera are employed (Kim et al. 2014). The market price of those high-speed video cameras typically is of the order of a few thousand to tens of thousands euros, which is often unaffordable for low-budget projects. This motivates us to search for a simple solution – an affordable stroboscopic imaging technique comprising of a regular PC, free software, a LED light source and a standard web camera. The experimental set-up is initially designed for studying resonant oscillations of droplets in the frequency range of up to 500 Hz and it was proven that it can suc-

cessfully replace the expensive high frame rate video cameras in studies of droplet shape oscillations.

### 2. STROBOSCOPIC EFFECT

The stroboscopic effect is an optical phenomenon based on temporal aliasing of signals due to the persistence of eye vision. (Coltheart, 1980 M., Van Veen, 1997). It has been used as early as the 1830's finding many applications in fundamental physics research and in industrial manufacturing as well (Van Veen, 1977). By permitting an intermittent observation of a cyclically moving object, in such a way as to produce an illusion of slowed or stopped motion, the stroboscopic technique allows the qualitative and quantitative research on kinematic properties such as trajectory, velocity and acceleration at equidistant time intervals (Van Veen, 1977; Yang, 2001; Nedev et al. 2009; Kubota, 1983; Blanc et al. 1981). Independent of motion type, one may use a high-speed video camera capable of capturing from a few hundred to thousands of frames per second. In the case of repetitive motion like harmonic oscillations, an affordable alternative set-up could be built, comprising of a flickering light source and a standard webcam. The concept of this technique is shown in Fig. 1.

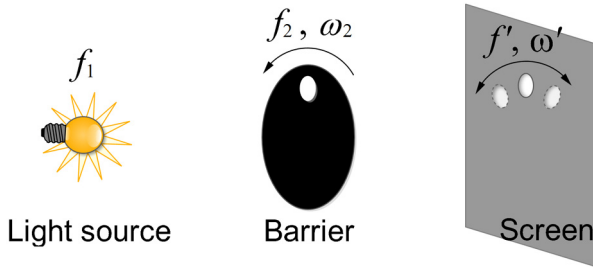


**Fig. 1.** Stroboscopic technique for studying fast rotating objects with a flickering light source.

The barrier is a disk rotating with constant angular frequency  $\omega_2 = 2\pi f_2$  and a hole in its periphery allows light to travel through and generate an image of the hole on the screen. The image appears to rotate with an angular frequency  $\omega' = 2\pi f'$  determined by the difference  $\Delta f = f_2 - f_1 = f'$  between the rotational frequency  $f_2$  of the barrier and the flashing frequency  $f_1$  of the light source. If  $f_1 = f_2$ ,  $f'$  is zero and the image appears stationary. The frequency  $f'$ , the period  $T'$  and the angular frequency  $\omega'$  of the image can be calculated as follows:

$$f' = \Delta f = f_2 - f_1 = \frac{\omega_2}{2\pi} - f_1 \quad (1)$$

$$T' = \frac{1}{f'} = \frac{1}{f_2 - f_1} = \frac{2\pi}{\omega_2 - 2\pi f_1} \quad (2)$$

$$\omega' = \frac{2\pi}{T'} = \omega_2 - 2\pi f_1 \quad (3)$$

When the flashing frequency  $f_1$  is near, but not at such synchronism ( $f_2 > f_1$ ), a slow-motion replica of the actual motion appears. Each successive flash occurs at a slightly later part of the cycle and the apparent slow motion is in the same direction as the actual motion. On the contrary, if ( $f_2 < f_1$ ), the apparent motion is in the reverse direction (Van Veen, 1977). This approach is used in our study of droplet shape oscillations. By illuminating the droplets, the apparent image is captured with a regular video camera, capable of up to 30 fps, resulting in capturing up to 30 images per second of a single stroboscopic position.

### 3. DROPLET SHAPE OSCILLATIONS

The oscillating drop technique, for measuring properties of liquids and studying the interface of a droplet, has been analyzed and reviewed widely in literature (Milne et al. 2014; Zografov et al 2014; Meier et al. 2000; Mettu et al. 2012). Most of the theoretical analyses are based on the pioneering work of Rayleigh, considering resonant modes of an ideal liquid sphere (Rayleigh, 1882). The main parameter in those studies is the resonant frequency,  $f_n$ , of spherical droplets unaffected by external forces such as gravity. The resonant frequency depends on the resonant mode,  $n$ , the surface tension,  $\sigma$ , the radius,  $r$ , and the density of the droplet,  $\rho$ , so that:

$$f_n^2 = n(n-1)(n+2) \frac{\sigma}{4\pi^2 \rho r^3} \quad (4)$$

In the present work, resonant oscillations of pendant droplets excited by a dielectric force were studied. Forced oscillations disturb the equilibrium state of the droplet and the deviations (e.g. oscillation frequencies) are detected by an optical system comprising of a weak laser beam and a photodiode. Detailed description of the technique has been published elsewhere (Zografov et al., 2014; Tankovsky et al., 2011; Tankovsky et al., 2013). With the help of the proposed stroboscopic technique, images of droplet shapes in resonant modes  $n=2$  and  $n=3$  were observed.

### 4. MATERIALS AND METHODS

Nowadays, computers have embedded soundcards with qualities good enough to be implemented for scientific purposes in the acoustic frequency range (20 Hz to 20 kHz). Thus, they can be used as a cost-effective replacement of the expensive equipment in low budget projects. Our experimental setup includes (Fig. 2): a standard PC with an inbuilt audio card, an operational amplifier, a non-continuous light source (21-white LED array), the object of study – 1.5 mm in diameter oscillating water droplet, a standard webcam and free downloadable software.

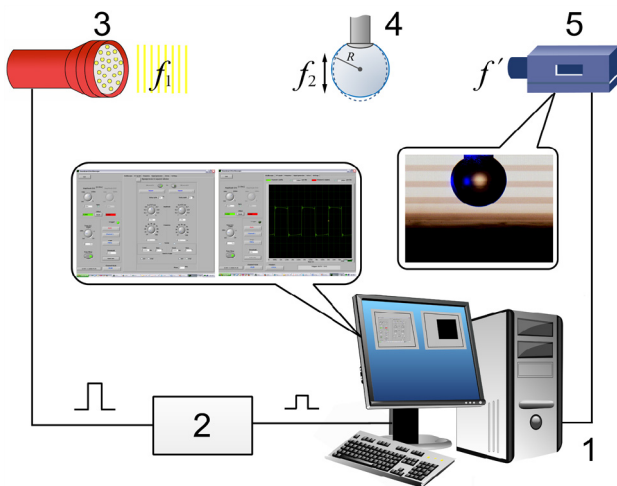


**Fig. 2.** Experimental setup: (1) standard PC, (2) audio amplifier, (3) 21-white LED array, (4) oscillating droplet, (5) standard webcam 25 fps.

The soundcard (Fig. 3) was used as a two-channel generator, which controls both, the frequency and duration of the light impulses emitted from the diodes. The maximum power consumption of the LEDs roughly amounts to 3,6 W ( $I = 400$  mA,  $V_{cc} = 9$ V) and required a dual power output amplifier (Fig. 4) which amplified the signal before transmitting it to the diode array. The light source was fixed on an optical mount and emitted white light directed at the droplet. The standard webcam was used for registering and sending real-time images. They may be either directly viewed or stored for further analysis. Its lens was replaced with a photographic one, coupled with the cam. The interior of the joint was matted black in order to avoid picking up deflected light from the inner walls. The compound optical system was finally fixed on an optical mount rail. The distance between the optical system and the droplet could be adjusted precisely by a micrometric screw, until an optimally focused image was obtained. The light source, the droplet and the optical components were aligned along the optical mount axis.

#### 4.1. Computer Sound Card

A soundcard – Realtek ALC622 was used. The ALC662 features three stereo DACs, two stereo ADCs, and legacy analog input to analog output mixing, to provide a fully-integrated audio solution for multimedia PC systems (<http://www.realtek.com.tw/products>).

In signal processing, sampling is the reduction of a continuous-time signal to a discrete-time signal. Therefore, a sample is a value or set of values at a point in time and/or space. For functions that vary with time, let  $s(t)$  be a continuous function (or “signal”) to be sampled, and let sampling be performed by measuring the value of the continuous function every  $T$  seconds, which is called the sampling interval or the sampling period. Then the sampled function is given by the sequence  $s(nT)$  for integer values of  $n$  (Weik, 1996).

The sampling frequency or sampling rate,  $f_s$ , is the average number of samples obtained in one second (samples per second), thus  $f_s = 1/T$ .

Reconstructing a continuous function from samples is done by interpolation algorithms (Rao, 2008). All our audio card DACs and ADCs support 44.1k/48k/96 kHz sample rates which is more than enough for the Nyquist-Shannon sampling theorem to be valid while working in the acoustic frequency range, allowing a precise reconstruction of signals (Shannon, 1949). Since the reconstruction of the signal was done by a DAC with physical limitations, deviations from the perfect mathematical case of reconstruction could be expected to occur. A variety of distortions such as aliasing, noise, aperture error, slew rate limit error and errors from quantization should be taken into account as well.

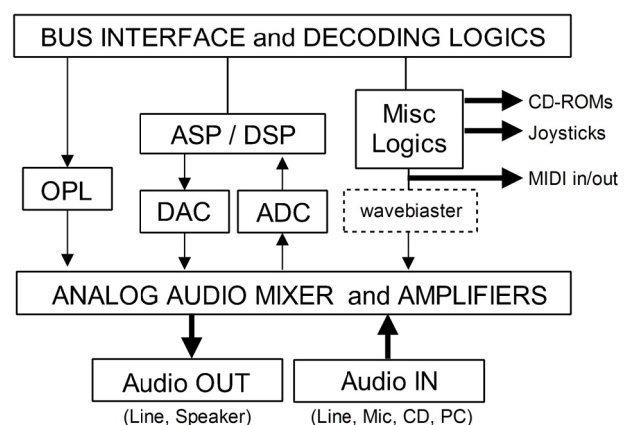


**Fig. 3.** Block diagram of sound card modules.

The signal to noise ratio of the Realtek is typical for a middle-class one and amounts to 98 dB. DACs and ADCs have a deviation of less than 0.02 dB in the frequency response.

The dynamic range is about 100 dB. The characteristics of the card greatly influence the performance of the white LEDs and a distortion in the signal shape can occur in case of poor quality soundcards. Fortunately, most inbuilt audio cards are good enough to support work in the acoustic range and especially in low frequency resonance oscillations of droplets. The soundcard serves as a two-channel generator and a two-channel receiver.

#### 4.2. Light Source and Amplifier

The light source used consists of 21 Cree 5 mm white LEDs with a minimum color temperature of 4600 K and a typical one of 9000 K (Datasheet, <http://www.cree.com>). The luminous intensity varies from 1100 – 4180 mcd and is 2750 mcd at a typical forward current of 20 mA per diode. The LEDs pulse response is in the microsecond range thus allowing them to emit light impulses in the MHz range (LED Frequency response, <http://www.jensign.com>). They turn out to be suitable emitters for studying low frequency processes.

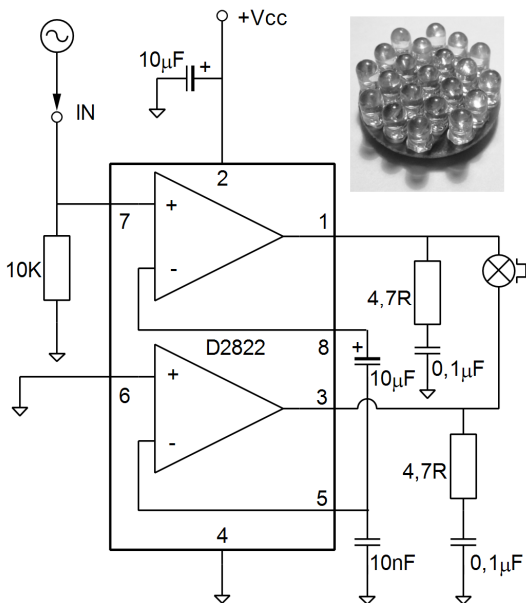


Fig. 4. LED array and the amplifier diagram.

The amplifier is a cheap dual power amplifier D2822 by Silicore, typically used in audio speakers (Dual power amplifier D2822, <http://pdf.datasheetcatalog.com>). It is used in a “Bridge test circuit”, supplying the LEDs power, which can’t be achieved with the soundcard alone.

#### 4.3. Web Camera

In the current set-up, a standard Intuix\_W1300 CMOS webcam was used. Having an image resolution of 1.3 MPx and 15-30 fps it perfectly suits our experimental needs.

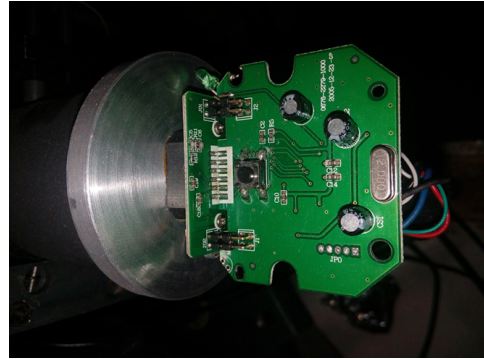


Fig. 5. Web camera assembly.

#### 4.4. Software

For controlling the frequency and the shape of the analog signals, generated by the LEDs controlling soundcard, specialized software is used. It controls the audio card using the operational system of the PC as a mediator and can be used as a functional two- channel generator and simultaneously as a two- channel oscilloscope. The Soundcard Oscilloscope software, written by Christian Zeitnitz, is free of charge for non-commercial use and can be downloaded (Zeitnitz, <https://www.zeitnitz.eu>). The software input data is directly received from the soundcard with 44.1 kHz and a 16 Bit resolution. The frequency range depends on the sound card, but 20 – 20 000 Hz is accessible with all modern cards. In addition, the oscilloscope contains a two-channel signal generator of sine, square, triangular, saw tooth wave forms, and different noise spectra in the frequency range from 0 to 20 kHz. The signal can be given by a mathematical expression as well. Additional features are added such as Fourier analysis, X/Y graph which displays the two channels against each other (e.g. Lissajous figures can be produced), a Waterfall graph function, which displays frequency analysis and many other. The software requirements are a standard Windows operational system and a soundcard, which makes it applicable to almost any modern PC.

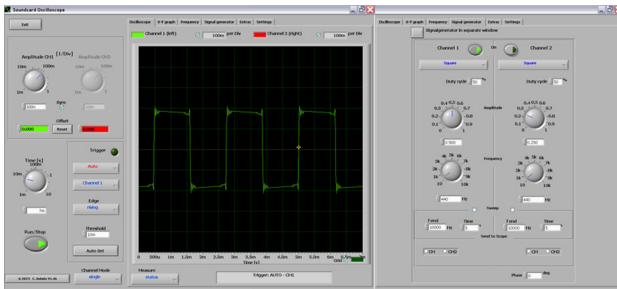


Fig. 6 Zeitnitz V1.46 control interface (Zeitnitz C., [https://www.zeitnitz.eu/scope\\_en](https://www.zeitnitz.eu/scope_en))

## 5. RESULTS AND DISCUSSION

Resonant oscillations of a pendant droplet (deionized water) were studied in the range of 30 to 300 Hz. Resonant shape oscillation modes  $n=2$  and  $n=3$ , were observed and captured using the proposed simple stroboscopic technique. The size of the examined droplet is in the millimeter range keeping the droplet Bond number less than 1.

In Fig. 7, we can clearly recognize the typical shape for mode  $n=2$ , with maximal (a) and minimal elongation (b) of the droplet. The captured images of resonant mode  $n=3$ , with maximal (a) and minimal elongation (b), are shown in Fig. 8. The observed shapes are in agreement with the vibration modes predicted by Chiba et al. (Chiba et al., 2012) in case of an anchored edge meniscus.

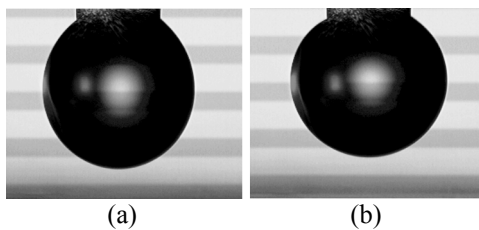


Fig. 7. Water droplet  $r = 0,890$  mm: resonant mode  $n = 2$ , at  $f = 80$  Hz.

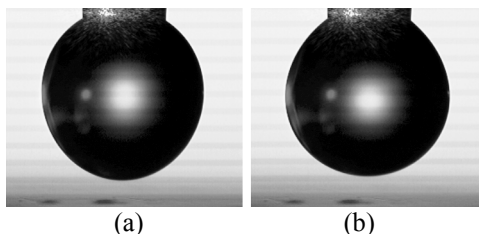


Fig. 8. Water droplet  $r = 0,910$  mm: resonant mode  $n = 3$ , at  $f = 155$  Hz.

The obtained results confirm that the proposed simple and affordable technique is a

fully functional tool for studying resonant droplet shape oscillations and can successfully replace the expensive high-speed cameras in case of a limited budget.

## ACKNOWLEDGEMENTS

We would like to warmly thank the University of Sofia student council for graciously funding our participation in the Fifth National Student Conference of Physics in Plovdiv where our work was presented. We would also like to thank “The Science Team Project”, whose help has proved invaluable for conducting the described experiments (<http://phys.uni-sofia.bg/~zoggy/sciteam/>).

## REFERENCES

- Blanc, R. H., & Giacometti, E., 1981. Infrared stroboscopy – a method for the study of thermomechanical behaviour of materials and structures at high rates of strain, *Int. J. Solids Struct.*, 17(5), 531–540.
- Chiba, M., Michiue, S., & Katayama, I., 2012. Free vibration of a spherical liquid drop attached to a conical base in zero gravity; *J. Sound Vib.*, 331, 1908–1925.
- Coltheart, M., 1980. The persistences of vision, *Philos Trans R Soc Lond B Biol Sci.*, 290(1038), 57–69.
- Cree LED Datasheet  
<http://www.cree.com/~media/Files/Cree/LEDComponents-and-Modules/HB/Data-Sheets/C535A-WJN-877.pdf>
- Deepu, P., Basu, S., Kumar, R., 2014. Multimodal shape oscillations of droplets excited by an air stream, *Chem. Eng. Sci.* 114, 85–93.
- Dual power amplifier D2822 datasheet  
[http://pdf.datasheetcatalog.com/datasheets/105/373757\\_DS.pdf](http://pdf.datasheetcatalog.com/datasheets/105/373757_DS.pdf)
- Kim, H., Yang, J., & Chung J., 2014. Resonant oscillation phenomena of a sessile droplet on electrohydrodynamic jetting nozzle, *Japanese Journal of Applied Physics*, 53, 05HC03.
- Kubota, Y., *United States Patent* 4,380,026 / 12.04.1983 LED Frequency response  
<http://www.jensign.com/Discovery/LEDFrequencyResponse/>
- Meier, W., Greune, G., Meyboom, A., & Hofmann K.P., 2000. Surface tension and viscosity of surfactant from the resonance of an oscillating drop, *Eur. Biophys. J.*, 29, 113–124.
- Mettu, S., & Chaudhury M. K., 2012. Vibration Spectroscopy of a Sessile Drop and Its Contact Line, *Langmuir*, 28, 14100–14106.
- Milne, A. J. B., Defez, B., Cabrerizo-Vílchez, & M., Amirfazli, A., 2014. Understanding (sessile/constrained) bubble and drop oscillations, *Adv. Colloid Interface Sci.*, 203, 22–36.

- Nedev, K., Cholakov, P., Iliev L., Saeva D., 2009. Mechanics – laboratory practice, *Univerisity Press St. Kliment Ohridski* (in Bulgarian language), 42–49.
- Noblin, X., Buguin, A., & Brochard-Wyart F., 2005. Triplon Modes of Puddles; *PRL* 94, 166102.
- Oh, J.M., Ko, S.H., & Kang K.H., 2008. Shape Oscillation of a Drop in ac Electrowetting, *Langmuir*, 24, 8379–8386.
- Rao, K.U., 2008. Signals and Systems. *I K International Publishing Hous*, 576 pp. ISBN 8189866893.
- Rayleigh L., 1882. On the equilibrium of liquid conducting masses charged with electricity, *Philos. Mag.*, 14, 184–186.
- Realtek ALC662 audiocard  
<http://www.realtek.com.tw/products>
- Shannon C.E., 1949. Communication in the presence of noise, *Proc. IRE*, 37(1), 10–21.
- Tankovsky, N., Zografov, N., & Russev S., 2013. Electrically Driven Resonant Oscillations of Pendant Hemispherical Liquid Droplet and Possibility to Evaluate the Surface Tension in Real Time, *Z. Phys. Chem.*, 227(12), 1759–1766.
- Tran, S.B.Q., Byun, D., Yudistira, H., & Oh, J.H., 2011. Semianalytical study of hemispherical meniscus oscillation with an anchored edge on a conductive flat plate under an AC electric field, *Phys. Fluids*, 23, 022006.
- Van Veen, F., 1997. Handbook of Stroboscopy, GenRaf Inc. USA, 93 pp.
- Weik M.H., 1996. Communications Standard Dictionary, *Springer*, pp. 1192, ISBN 0412083914.
- Yang, W.-J., 2001. Handbook of Flow Visualization. *CRC Press*, 272 pp.
- Young-Sub, S., & Hee-Chang, L., 2014. Shape oscillation and detachment conditions for a droplet on a vibrating flat surface; *Eur. Phys. J. E*, 37, 74.
- Zeitnitz, C., [https://www.zeitnitz.eu/scope\\_en](https://www.zeitnitz.eu/scope_en)
- Zografov, N., & Tankovsky, N., 2013. Examination of the liquid-air interface properties by oscillating pendant droplet under electric field influence technique – a Q-factor approach, Annual reports of SU, Faculty of Physics, 107, 103–112.
- Zografov, N., Tankovsky, N., & Andreeva, A., 2014. Droplet oscillations driven by an electric field, *Colloids and Surf A: Physicochem. Eng. Asp.*, 460, 351–354.
- Tankovsky, N., & Zografov, N., 2011. Oscillations of a hanging liquid drop, driven by interfacial dielectric force, *Z. Phys. Chem.*, 225(4), 405–411.